Macroscopic chimeralike behavior in a multiplex network

Nikita S. Frolov,[1,2] Vladimir A. Maksimenko,[1] Vladimir V. Makarov,[1] Daniil V. Kirsanov,[1]
Alexander E. Hramov,[1] and Jürgen Kurths[2,3,4]

[1]*Research and Educational Center "Artificial Intelligence Systems and Neurotechnology," Yuri Gagarin State Technical University of Saratov, Saratov 410054, Russia*
[2]*Potsdam Institute for Climate Impact Research, 14473 Potsdam, Germany*
[3]*Department of Physics, Humboldt University, 12489 Berlin, Germany*
[4]*Institute for Complex Systems and Mathematical Biology, University of Aberdeen, Aberdeen AB24 3UE, United Kingdom*

(Received 21 April 2018; published 30 August 2018)

In this paper we study the dynamics of a multiplex multilayer network, where each layer is composed of identical Kuramoto-Sakaguchi phase oscillators with nonlocal coupling. We focus on a three-layer multiplex network and observe a specific form of multiplex network behavior, the macroscopic chimeralike state. It is decomposed by a splitting of the layers with initially close dynamics into subgroups. The first group consists of two layers performing one type of dynamics, whereas the rest perform the other type, after the introduction of interlayer coupling. Based on an intensive computational analysis, we show that areas of macroscopic chimeralike states are observed close to the critical transition points of intralayer (microscopic) states in the parameter space. We find that this macroscopic chimeralike state is excited at weak and medium interlayer coupling strength, wherein the interlayer phase lag here plays an important role, since this is a network parameter which controls macroscopic dynamics and transforms boundaries between intralayer states. The obtained numerical results are validated analytically by considering the multiplex network dynamics using the Ott-Antonsen reduction of the governing network equations.

DOI: 10.1103/PhysRevE.98.022320

I. INTRODUCTION

The chimera state discovered by Kuramoto and Battogtokh [1] and proven theoretically by Abrams and Strogatz [2] is a specific form of a nonlinear oscillator ensemble behavior which manifests as a network symmetry breaking and split into coexisting populations of synchronous and desynchronized elements. Since that time the phenomenon of chimera behavior has excited significant interest and has given rise to numerous theoretical and experimental works (see the review on chimera states by Panaggio and Abrams [3]). In this framework, chimera patterns have been observed in various systems, e.g., laser networks [4,5], neural ensembles [6–9], and coupled chemical [10–12], mechanical [13–17], and electronic oscillators [18–20]. Despite the significant progress made on the way to understanding the nature of chimera states and its possible applications in science and technology plenty of challenging tasks still remain poorly studied.

Typically, when studying properties of chimera states, complex networks are studied whose nodes contain single nonlinear oscillators coupled according to different link topologies. However, we suppose that it could also be interesting to analyze similar effects in networks whose nodes themselves are complex subnetworks. Such a network topology could be a relevant model to describe many real-life systems, which exhibit complex organization and hierarchical structure, e.g., transportation networks [21], population networks [22], social networks [23], and functional network of brain cortex [24]. In this framework, the interaction between subnetworks reflects macroscopic properties of the whole network, while the processes of self-organization and structure formation taking place inside each subnetwork are considered as microscopic properties of the whole network [25]. Thus, the issue related to macrolevel pattern formation analysis essentially follows from the nature of such networks and has been poorly studied so far. Previously, Martens [26] studied chimera states in a triangular network, which is the simplest network topology that demonstrates chainlike and ringlike properties and consists of three subpopulations. It has been shown that along with all-coherent and all-incoherent group behavior such a system demonstrates two stable chimera attractors, which are associated with the coexistence of coherent and incoherent groups and are born through a saddle-node bifurcation.

Another interesting concept of complex network topology when subnetworks are interconnected and interact with each other is multilayer multiplex networks [27–29]. In the framework of this approach to complex network construction, subnetworks are represented as isolated layers, where an individual node takes part in several layers simultaneously. Such network topology reflects properties of many real-life and complexly organized systems, for example, the neural network of the brain cortex, where each layer represents network dynamics corresponding to different brain rhythms [30]. Recent studies of chimera pattern interactions formed at different levels of a two-layer multiplex network [31,32] have shown that, depending on the value of interlayer coupling, chimera patterns could be either excited or suppressed. In these works authors analyzed mostly microlevel network dynamics, taking into account only chimera pattern properties individually on each layer of the multiplex network.

The discovered effects raise important questions. Namely, is it possible to observe a chimera state on the macroscopic level of the multilayer multiplex network? In other words, does multiplex topology allow for a macroscopic chimera or chimeralike state in a similar way as observed by Martens in the case of a triangular network? Finding such regimes of multiplex network behavior characterized by a macroscopic level symmetry breaking, when the subnetworks located at different layers split into different spatiotemporal patterns, would widen the view on the phenomenon of the chimera state, which was originally discovered for a single group of interacting nonlinear oscillators. In this context we call this phenomenon a macroscopic chimera.

This work aims at studying regimes of macroscopic chimeralike behavior under the interaction between identical layers in a three-layer network coupled by multiplexing. In particular, we have found long-living macroscopic chimera attractors, which appear in the formation of different spatial patterns on different network layers. Finding and examining the macroscopic chimera regimes is relevant in the context of a deeper understanding of complex systems described in the framework of multiplex models. Along with the finding of such chimeralike regimes in multiplex networks, we infer the relations between microscopic and macroscopic self-organization processes.

This paper is organized as follows. We state the model equations and describe its main properties in Sec. II A. Additionally, a detailed description of the method for estimation of layer coherence degree is outlined in Sec. II B. Next, in Sec. III, we discuss the results of our numerical simulations and describe the phenomenon of a macroscopic chimeralike behavior, along with analyzing the emergence of macroscopic chimera dependent on network control parameters. In Sec. IV we validate the obtained numerical results on the macroscopic chimera regime in the framework of the Ott-Antonsen reduction [33,34]. Finally, we summarize and discuss the results of macroscopic chimera in Sec. V.

II. MATHEMATICAL MODEL AND METHODS

A. Multilayer network model

The multilayer multiplex networks under study consist of $L = 3$ layers, each having $N = 100$ nodes, as schematically represented in Fig. 1(a). One can notice that each node of the multiplex network performs two types of coupling: intralayer (solid lines) and interlayer (dashed lines). The dynamics of the nodes is described by identical Kuramoto-Sakaguchi (KS) equations, which are paradigmatic models allowing for chimera patterns,

$$\frac{d\phi_i^l}{dt} = \omega_0 - \frac{\lambda_1}{2R_c}\sum_{r=i-R_c}^{r=i+R_c}\sin\left(\phi_i^l - \phi_r^l + \alpha_1\right) + \frac{\lambda_2}{2}\sum_{k\neq l}\sin\left(\phi_i^l - \phi_i^k + \alpha_2\right), \quad (1)$$

where ϕ_i^j is the phase of the ith KS oscillator on the jth layer, ω_0 is the natural frequency, λ_1 and λ_2 are the strengths of intra- and intercoupling, respectively, R_c is the radius of the nonlocal intralayer coupling, and α_1 and α_2 are the coupling phase lag corresponding to intra- and interlayer coupling, respectively. Here the subscripts denote the number of KS oscillators and superscripts denote the number of layers. It should be noted that $\phi_{-i}^j = \phi_{N_0-i}^j$. The second term on the right-hand side in Eq. (1) stands for a nonlocal intralayer coupling and the third one determines a multiplex all-to-all interlayer coupling. Without loss of generality, we set $\omega_0 = 0$ throughout the study.

The initial phase distribution has been chosen in the form of a cosine wave, which is slightly shifted on each layer with respect to the others:

$$\phi_i^l(0) = -\pi\cos\left(2\pi\frac{i-l}{N}\right). \quad (2)$$

This initial condition set allows for a microscopic chimera pattern formation.

To reduce the number of network control parameters, let us fix the coupling radius $R_c = 35$ and the coupling strength $\lambda_1 = 0.085$, which determine the intralayer coupling properties. In this case, the microscopic dynamics of each single layer is controlled by only one parameter, the coupling phase lag α_1. As we will show below, an increase of α_1 from 1.4 to 1.6 leads to the transition from a synchronous layer dynamics to desynchronization of layer nodes through the birth of a partially synchronized chimera state.

Based on the knowledge of microscopic KS layer properties dependent on the control parameter α_1, we return to the entire network, which consists of three identical layers coupled by multiplexing. It should be noted that the term "identical" means that all the layers of the multiplex network are described in terms of identical mathematical equations (1) with identical control parameters but slightly mismatched initial phase distributions (2). Let us denote hereinafter the macroscopic states of the network with three capital letters, each of which reflects the type of microscopic state on each layer of the network, e.g., SSS denotes the network state, where all layers perform a synchronized behavior on the microscopic level.

B. Coherence measure

To describe the collective behavior of the multiplex network, we introduce the coherence measure (CM) based on the layer recurrence matrix construction, which shows the coherence level individually for each layer. Generally, the recurrence-based methods are used to analyze time-dependent data and to find a time-series correlation in the time domain [35]. Inspired by the recurrence-based methods, we propose an approach to measure the spatial correlation in the network of interacting oscillators and classify intralayer states. It should be noted that our approach is relative to the method for classification of chimera states recently proposed by Kemeth [36]. However, in our approach we use the recurrence matrix to estimate local coherence in the subgroup of each layer element and afterward calculate the total CM to characterize the whole layer state. Thus, the CM represents a relative size of coherent subpopulation within a single layer of the multiplex network.

Following [35], to determine the CM, we start with the calculation of the network recurrence matrix

$$R_{ij} = H(\varepsilon - |\phi_i - \phi_j|), \quad (3)$$

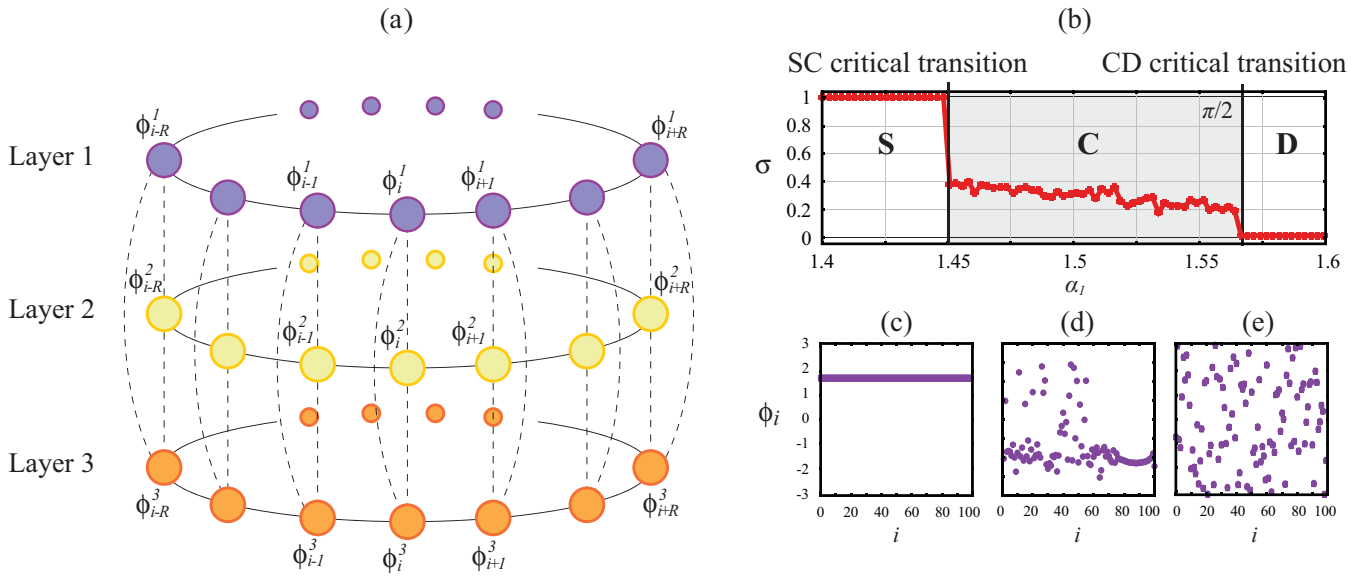

FIG. 1. (a) Schematic illustration of a three-layer multiplex network of Kuramoto-Sakaguchi oscillators with a nonlocal intralayer coupling and a global interlayer coupling [Eq. (1)]. (b) Dependence of coherence measure σ [Eq. (5)] on the controlling parameter α_1 for a single network layer with the following parameters: $\lambda_1 = 0.085$ and $R_c = 35$. Bold vertical lines indicate single-layer critical transitions: the synchronized-chimera transition at $\alpha_1 = 1.45$ and the chimera-desynchronized transition at $\alpha_1 = \pi/2$. Examples of different single-layer states corresponding to different regimes: (c) synchronized as S ($\alpha_1 = 1.42$), (e) chimera as C ($\alpha_1 = 1.52$), and (d) desynchronized as D ($\alpha_1 = 1.59$).

where H is the Heaviside function and the matrix element R_{ij} is equal to 1 if the state of the jth node of a layer lies in the ε neighborhood of the ith node. In Fig. 2(a) one can see that in the coherent part of the network layer phases of the KS oscillators are not precisely equal and form a curvature on the presented snapshot. Taking this into account, we set the threshold value $\varepsilon = 0.2$ to provide an appropriate calculation. Based on the obtained matrix R, one can compute the local coherence measure of the ith node (σ_i) by summing over a local neighborhood of the ith element

$$\sigma_i = \frac{1}{2\Delta} \sum_{j=i-\Delta}^{i+\Delta} R_{ij}, \tag{4}$$

where Δ is half the size of the ith local neighborhood. We have found that an appropriate estimation of σ_i is given if the size of the local neighborhood is a few percent of the size of the entire layer. Since we have considered $N = 100$ nodes within each layer, we set $\Delta = 3$ to give an appropriate estimation of the CM.

We demonstrate the process of CM estimation for the example of a chimeric single-layer network presented in Fig. 2(a). One can see in Fig. 2(b) that σ_i is close to 1.0 in the area corresponding to the coherent subpopulation (chimera state), but differs from 1.0 elsewhere.

Finally, one can determine the total coherence measure σ by summing those σ_i exceeding the threshold value δ over the ensemble

$$\sigma = \frac{1}{N} \sum_{i=1}^{N} H(\delta - \sigma_i). \tag{5}$$

According to the typical values which σ_i takes in coherent and incoherent subpopulations as presented in Fig. 2(b), we set $\delta = 0.7$.

In the framework of the proposed recurrence-based approach, the CM provides the estimation of the size of the synchronized part inside a single layer. Thus, $\sigma = 0$ corresponds to a totally desynchronized behavior within the layer, $\sigma = 1$ corresponds to a totally synchronized layer dynamics, and $0 < \sigma < 1$ indicates the formation of partially synchronous or chimera patterns as shown in Figs. 1(b)–1(d). Let us denote the microscopic states associated with synchronized, chimera,

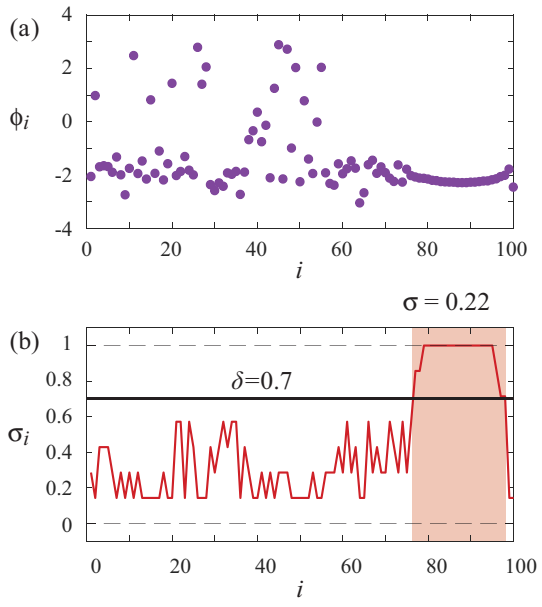

FIG. 2. (a) Typical pattern of the chimeric single-layer network observed at $\alpha_1 = 1.52$, $R_c = 35$, and $\lambda_1 = 0.085$. (b) Local coherence measure σ_i of the KS ensemble corresponding to the considered pattern shown in (a).

and desynchronized layer dynamics by single capital letters S, C, and D, respectively. Indeed, one can see in Fig. 1(b) that the single-layer dynamics undergoes two critical transitions under variation of the phase lag α_1. An increase of α_1 leads to the transition from a synchronous layer dynamics S [Fig. 1(c)] to desynchronization of the layer nodes D [Fig. 1(e)] through the birth of a partially synchronized chimera state C [Fig. 1(d)]. Namely, the transition from S to C is observed at $\alpha_1 = 1.45$ and the transition from C to D corresponds to $\alpha_1 = \pi/2$. In this particular case, the coherent subpopulation of the network layer includes 22 nodes and $\sigma = 0.22$. Thus, we can conclude that calculation of the CM provides a good estimation of the relative coherent group size of the network layer.

III. NUMERICAL RESULTS

To perform an accurate analysis of the considered three-layer multiplex network and solve the system of ordinary differential equations (1) numerically, we have used the fourth-order Runge-Kutta method. The calculations have been carried out by taking the integration time step as $dt = 0.01$.

Let us start the analysis from the case of weak interlayer coupling. In this situation, one can expect that the weak coupling between the layers, which exhibit close dynamical regimes, will contribute to either synchronization or desynchronization of interacting network layers with conservation of the dynamical properties within each layer. However, such regimes are rather trivial and understandable. In our study we focus on finding conditions which allow for a symmetry breaking on the macroscopic level of the considered three-layer network, i.e., when a group of two layers of the multiplex network exhibit similar dynamics, whereas for the rest one performs the other type of behavior. In this sense, we call such regimes macroscopic chimeralike regimes. We suppose that such chimeralike regimes can be observed in the neighborhood of microscopic critical transitions shown in Fig. 1(b). Figure 3 illustrates the transitions between different types of macroscopic behavior of the considered multiplex network under the variation of α_1 in the case of weak interlayer coupling $\lambda_2 = 0.005$ and a small value of interlayer phase lag $\alpha_2 = 0.5$. We see that the previously described expectations are justified and network macroscopic states, which are characterized by the establishment of similar microscopic states at all the layers, are represented in a wide range of α_1. In particular, the SSS state with $\sigma_1 = \sigma_2 = \sigma_3 = 1$ lies in the range $\alpha_1 \leqslant 1.44$, the DDD state in the range $\alpha_1 \geqslant 1.56$, and the CCC state corresponds to $\alpha_1 \in [1.4575, 1.5575]$. These ranges are characterized by a long-living (at least during a few thousand time units) macroscopic state. At the same time, one can see the excitation of macroscopic chimeralike states in two rather narrow areas: (i) at the boundary between SSS and CCC ($\alpha_1 \in [1.4425, 1.455]$) and (ii) at the boundary between CCC and DDD ($\alpha_1 \in [1.5525, 1.5575]$). We note that in the first region chimeralike states consist of coexisting chimeric and synchronized layers (CSS and CCS states), whereas the second one is composed of one chimera layer and two desynchronized layers (the CDD state). Surprisingly, we have not observed CCD states in the considered multiplex system; CCD states, initiated after switching the interlayer coupling, typically collapsed into either CDD or DDD states.

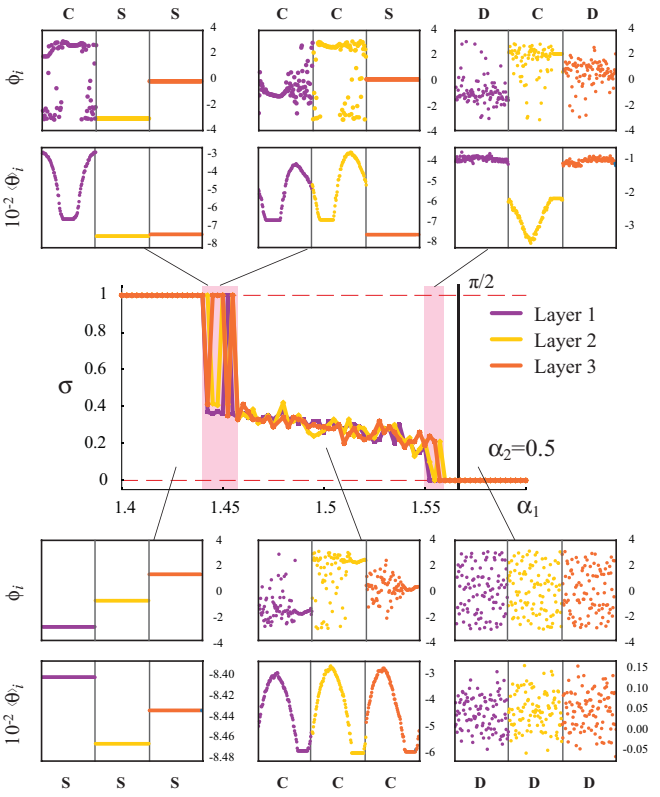

FIG. 3. Dependences of the coherence measure σ calculated for each layer of the multiplex network on intralayer phase lag α_1 under weak interlayer coupling $\lambda_2 = 0.005$ in the case of a low value of interlayer phase lag $\alpha_2 = 0.5$. The snapshots of the phase ϕ_i and mean phase velocity $\langle\theta\rangle_i$ of the multilayer network are taken at 7000 time units after introduction of interlayer coupling.

It is important to note that these chimeralike states are also long living. Based on this observation, one can conclude that these chimeralike states, CSS, CCS, and CDD, appear as some intermediate states at the boundary between the completely symmetric macroscopic states. In these narrow areas the chimeralike behavior on the macroscopic level of the network is excited due to the overlapping of regions of neighboring microscopic states under an interlayer interaction. The latter causes multistability of microscopic states, namely, the coexistence of two types of microscopic states: S and C in the case of CSS and CCS states and C and D in the case of the CDD state. The described chimera states become suppressed under the increase of the interlayer phase lag α_2 in the case of a weak interlayer coupling (Fig. 4). It can be clearly seen that the macroscopic chimera areas vanish at $\alpha_2 = 2.2$. Moreover, the SSS and DDD states perform an interlayer coherence at high values of α_2. We determine interlayer coherence as equality of node phase and mean phase velocity on each layer ($\phi_i^1 = \phi_i^2 = \phi_i^3$ and $\theta_i^1 = \theta_i^2 = \theta_i^3$).

An increase of the interlayer coupling strength λ_2 significantly changes the multiplex network dynamics. Figure 5 shows the transitions between the macroscopic states of the network under variation of α_1 for increasing $\lambda_2 = 0.02$. In particular, one can see from Fig. 3 that at low values of $\alpha_2 = 0.5$, the increase of λ_2 suppresses the macroscopic chimera

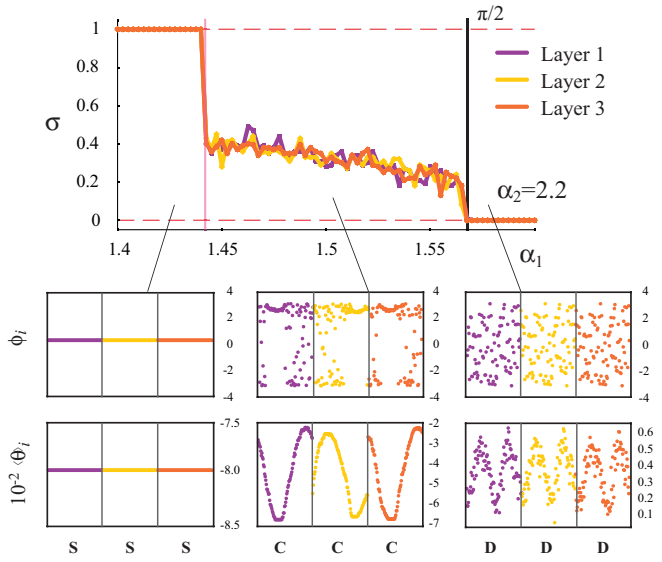

FIG. 4. Dependences of the coherence measure σ calculated for each layer of the multiplex network on the intralayer phase lag α_1 under weak interlayer coupling $\lambda_2 = 0.005$ in the case of a high value of interlayer phase lag $\alpha_2 = 2.2$. The insets illustrate various states emerging in the multilayer network in different ranges of control parameters. The snapshots of the phase ϕ_i and mean phase velocity $\langle\theta\rangle_i$ of the multilayer network are taken at 7000 time units after introduction of interlayer coupling.

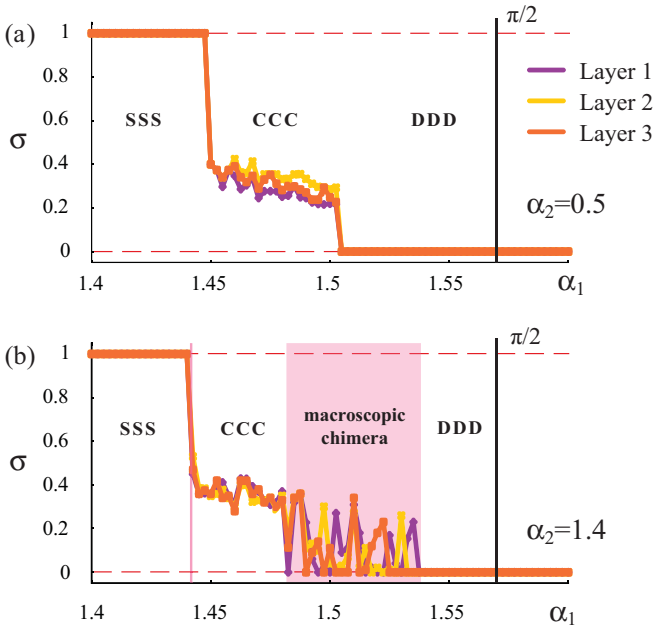

FIG. 5. Dependences of the coherence measure σ calculated for each layer of the multiplex network on intralayer phase lag α_1 under interlayer coupling strength $\lambda_2 = 0.02$ in the cases of (a) a low value of interlayer phase lag $\alpha_2 = 0.5$ and (b) a higher value of interlayer phase lag $\alpha_2 = 1.4$.

state in the multiplex network and considerably widens the area of the DDD state. Here the boundary between the CCC and DDD states shifts to $\alpha_1 \approx 1.5$ instead of $\pi/2$ in the uncoupled case. At the same time, the macroscopic chimeralike state of the multiplex network appears at higher values of α_2 [Fig. 5(b)], where $\alpha_2 = 1.4$. It can be clearly seen that in this case only the CDD-type chimeralike state with coexisting chimeric and desynchronized layers survives in the network. One can also see that the parameter range associated with excitation of macroscopic chimera behavior at $\lambda_2 = 0.02$ is significantly expanded in relation to the previously considered weak coupling case.

The introduction of strong interlayer coupling totally suppresses the formation of chimeralike behavior in the multiplex network. Figure 6 illustrates the transitions between macroscopic states for a strong interlayer coupling $\lambda_2 = 0.1$. In this case, we find an abrupt transition from the SSS state directly to the DDD state at $\alpha_2 < \pi/2$. In addition, at $\alpha_2 \geqslant \pi/2$ all the layers of the multiplex network perform interlayer coherence, where each element is synchronized with the same elements in the other layers under the influence of strong interlayer coupling. Note that the boundaries between macroscopic states in the case of strong interlayer coupling and high values of α_2 correlate well with boundaries between microscopic states obtained for a single layer. Taking the latter into account, one can conclude that interlayer synchronization forces the multiplex network to induce dynamical properties, which are close to the single-layer behavior.

Finally, we analyze the network behavior and evolution of the boundaries between different macroscopic states in a wide range of control parameters in more detail via the map of dynamical regimes on the plane (α_1, α_2) under increasing interlayer coupling λ_2 (Fig. 7). We uncover that weak interlayer coupling [Fig. 7(b)] does not significantly transform the boundaries compared to the uncoupled case [Fig. 7(a)]. It

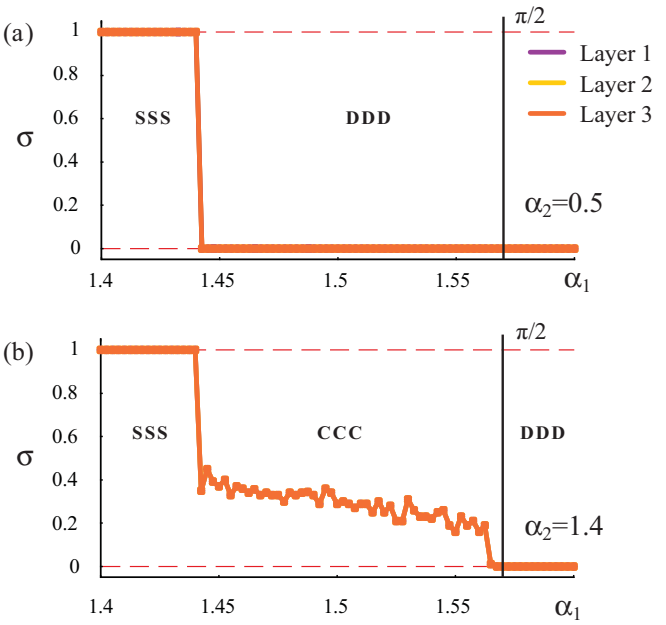

FIG. 6. Dependences of the coherence measure σ calculated for each layer of the multiplex network on the intralayer phase lag α_1 under strong interlayer coupling $\lambda_2 = 0.1$ in the cases of (a) a low value of interlayer phase lag $\alpha_2 = 0.5$ and (b) a higher value of interlayer phase lag $\alpha_2 = 1.4$.

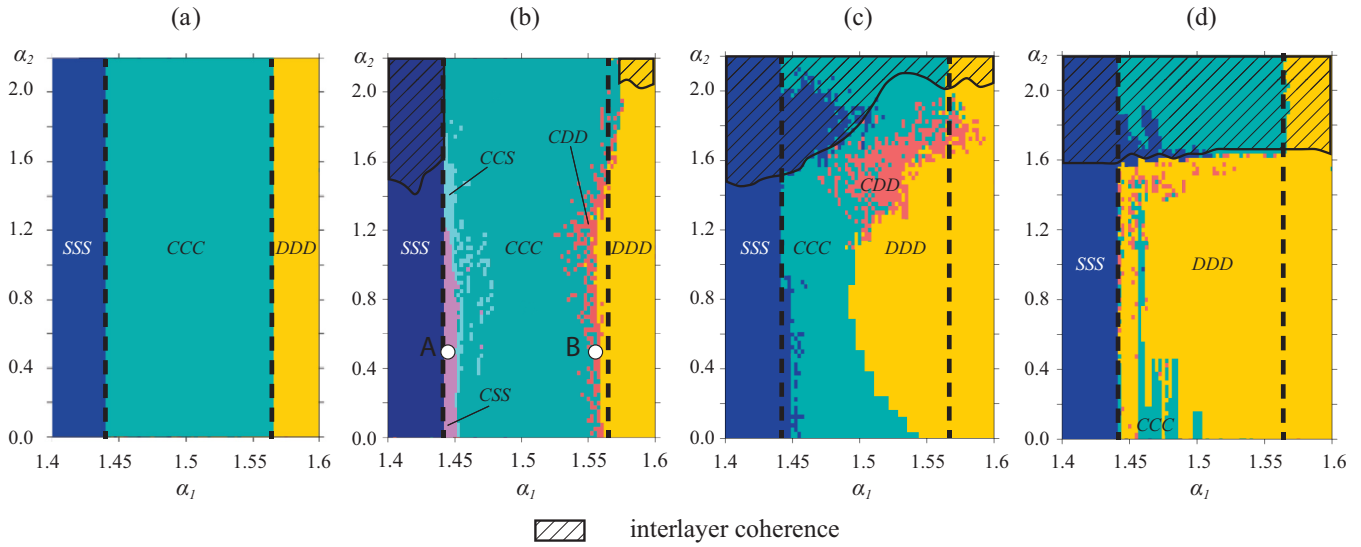

FIG. 7. Maps of multiplex network dynamical regimes on the parameter plane (α_1, α_2) for different values of interlayer coupling λ_2: (a) $\lambda_2 = 0$, (b) $\lambda_2 = 0.005$, (c) $\lambda_2 = 0.02$, and (d) $\lambda_2 = 0.1$. Dashed vertical lines indicate boundaries between microscopic states of the network. Colors indicate different macroscopic states of the multilayer network. The dynamics of the network at points A and B is considered in the framework of Ott-Antonsen reduction, which is illustrated in Fig. 8.

only allows for the occurrence of narrow macroscopic chimera areas in the neighborhood of the boundaries. We note that the macroscopic chimera region with coexisting C and S states is divided into CSS and CCS areas. It is essential that the CSS area is located close to the SSS region and CCS in turn is close to CCC. In the case of weak coupling, the boundary of the DDD state becomes slightly twisted with respect to the same boundary in the uncoupled case. The increase of the interlayer coupling strength, as shown in Fig, 7(c), makes the twisting of the boundaries more pronounced. The twisting of the DDD boundary overlaps the CCC region in the area of low α_2 and twisting of the SSS boundary overlaps the CCC area at high values of α_2. The area of the macroscopic chimeralike behavior of the network moves to the area of higher values of α_2 and vanishes at the boundary between SSS and CCC states. It can be clearly seen that an interlayer coupling increase contributes to the growth of the macroscopic chimera area. It should be noted that at $\lambda_2 = 0.02$ the region of interlayer coherence expands on a larger area in the plane (α_1, α_2) compared to the previously considered case of weak coupling. In the case of strong interlayer coupling at $\lambda_2 = 0.1$ [Fig. 7(d)], the boundaries become extremely twisted, so the DDD area almost totally overlaps the CCC area. At the same time the boundary of the interlayer coherence regime converges to the horizontal line, namely, $\alpha_2 \approx \pi/2$. Moreover, macroscopic chimeralike behavior is suppressed under a strong interlayer coupling.

Based on the observation of dynamical regime evolution in the (α_1, α_2) plane, we conclude that the formation of macroscopic chimeralike patterns in multilayer multiplex networks, as a specific state of networks with coexisting types of different microscopic states on different layers of the network, requires the overlapping of neighboring dynamical areas near the boundary between them. Such overlapping takes place due to the introduction of an interlayer phase lag at weak and medium interlayer coupling. Strong coupling leads to an extreme twisting of the boundaries and an almost total overlapping, which suppresses the formation of chimeralike regimes.

In addition, in the considered system a long-living combination of all three microscopic states within the network (for example, the SCD state) is impossible since the points of microscopic critical transitions and corresponding macroscopic boundaries are widely spaced in the α_1 range. Therefore, even introduction of the interlayer phase lag α_2 does not contribute to the intersection of all three microscopic states in some area of the (α_1, α_2) parameter plane.

IV. OTT-ANTONSEN REDUCTION

To prove the results of our numerical study and expand them to the case of an infinitely large number of oscillators on each layer, we turn to a description of the multiplex network in the form of the Ott-Antonsen (OA) ansatz [33,34]. We derive the equations in the form of the OA ansatz following [31]. Taking into account Euler's formula $e^{ix} = \cos(x) + i \sin(x)$, one can rewrite the governing equations of the three-layer multiplex network (1) in the form

$$\frac{d\phi_i^l}{dt} = \omega_0 + \mathrm{Im}\left[Z_i^l(t) e^{-i\phi_i^l}\right], \tag{6}$$

where the mean field Z_i^l is

$$Z_i^l(t) = \frac{\lambda_1}{2R_c} \sum_{k=i-R_c}^{r=i+R_c} e^{i\phi_r^l} e^{-i\alpha_1} - \frac{\lambda_2}{2} \sum_{k \neq l} e^{i\phi_i^k} e^{-i\alpha_2}. \tag{7}$$

As we consider the limiting case of an infinitely large number of oscillators on each layer $N \to \infty$, the dynamics of the lth layer is described by the probability density function $f^l(x, \phi, t)$, which conforms to the continuity equation

$$\frac{\partial f^l(x,\phi,t)}{\partial t} + \frac{\partial}{\partial \phi}\left(f^l(x,\phi,t) v^l(x,\phi,t)\right) = 0, \tag{8}$$

where

$$v^l(x,\phi,t) = \frac{d\phi}{dt} = \omega_0 + \mathrm{Im}[Z^l(x,t)e^{-i\phi}]. \quad (9)$$

It should be noted that Z^l in (9) is a mean field, rewritten in the continuous form

$$Z^l(x,t) = \int_0^1 \lambda_1 G(x-y)\int_0^{2\pi} f(x,\phi,t)e^{i\phi}e^{-i\alpha_1}d\phi\,dy - \frac{\lambda_2}{2}\sum_{k\neq l}\int_0^{2\pi} f(x,\phi,t)e^{i\phi}e^{-i\alpha_2}d\phi. \quad (10)$$

Here $G(\Delta) = H(\cos(2\pi\Delta) - \cos(r_c 2\pi))$ is a nonlocal coupling kernel with coupling the radius $r_c = 0.35$ and $H(\cdot)$ is the Heaviside step function. We are looking for a solution of (8)–(10) in the form of a Fourier series, taking into account the OA ansatz

$$f^l(x,\phi,t) = \frac{1}{2\pi}\left[1 + \sum_{n=1}^{\infty}\overline{a}_l^n(x,t)e^{in\phi} + \text{c.c.}\right]. \quad (11)$$

Substituting (11) into (8)–(10) and introducing the replacement

$$\int_0^{2\pi} f^l(x,\phi,t)e^{i\phi}d\phi = u_l(x,t), \quad (12)$$

we finally obtain the governing equation to describe the dynamics of the considered multiplex network in the framework of the OA reduction

$$\frac{du_l}{dt} = -i\omega_0 u^l(x,t) + \frac{1}{2}\left[Z^l(x,t) - u_l^2(x,t)\overline{Z}^l(x,t)\right], \quad (13)$$

where $Z^l(x,t)$ is rewritten in the form

$$Z^l(x,t) = \lambda_1 e^{-i\alpha_1}\int_0^1 G(x-y)u_l(y,t)dy - \frac{\lambda_2}{2}e^{-i\alpha_2}\sum_{k\neq l}u_k(x,t). \quad (14)$$

The complex function $u^l(x,t)$ provides information about the local order parameter and the local phase as the modulus $|u^l(x,t)|$ and the argument $\psi(x,t) = \arg[u^l(x,t)]$, respectively.

Using the derived equations (13) and (14), we have proved the possibility of macroscopic chimeralike state excitation in the multiplex network in the case of an infinitely large number of oscillators, when each layer of the multiplex network represents a continuous medium. We have chosen points A and B on the parameter plane (α_1, α_2) under weak coupling [Fig. 7(b)], which appear at different boundaries, to illustrate the emergence of macroscopic chimeralike states in the limiting case of an infinitely large number of oscillators. In Fig. 8 we present the space-time evolution of the network at points A and B much after the introduction of weak interlayer coupling. We find that the OA model accurately predicts the same type of multiplex network dynamics on the macroscopic level, which was previously uncovered in the framework of a purely numerical investigation. It should be noted that the macroscopic chimeralike states considered in the continuous limit, both CSS and CDD, are stable

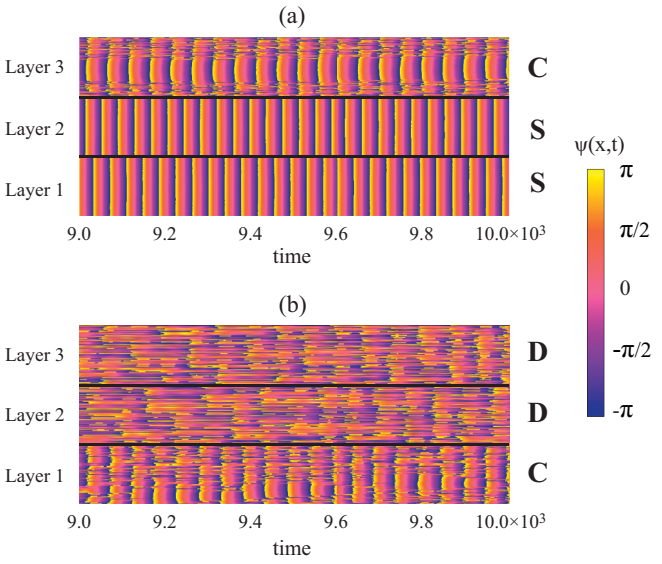

FIG. 8. Spatiotemporal evolution of the phase $\psi(x,t)$ obtained via numerical integration of Eqs. (13) and (14), which illustrates the regimes of stable macroscopic chimeralike behavior in the multiplex network. Here plots (a) and (b) correspond to points A and B in Fig. 5(b), respectively, and represent different macroscopic chimeralike patters. The control parameters are (a) $\alpha_1 = 1.445$, $\alpha_2 = 0.5$, and $\lambda_2 = 0.005$ and (b) $\alpha_1 = 1.555$, $\alpha_2 = 0.5$, and $\lambda_2 = 0.005$.

in time. Thus, consideration of the multiplex network in the framework of OA reduction proves the observation of long-living macroscopic chimeralike states in a finite-size network.

V. CONCLUSION

In this paper we have studied a phenomenon, the macroscopic chimeralike state, which emerges in multilayer multiplex networks. In particular, we have focused on consideration of a three-layer multiplex network, where each layer is composed of identical Kuramoto-Sakaguchi phase oscillators with nonlocal coupling. We have uncovered that this phenomenon consists in a split of the layers with initially close dynamics into subgroups, where the group of two layers performs one type of dynamics and the rest exhibit the other type, after the introduction of interlayer coupling. Based on the provided numerical analysis, we reveal conditions which allow for macroscopic chimera state emergence. In particular, we have observed that the macroscopic chimera state of the multiplex network is excited at weak and medium interlayer coupling strength. The interlayer phase lag plays here an important role since this is a network parameter which controls macroscopic behavior and transforms boundaries between intralayer states. According to the transformation of the boundaries between intralayer states, there appear areas of overlapping microscopic states close to the intralayer critical points that conditions the multistable macroscopic states of the multiplex network, namely, macroscopic chimera behavior. In turn, the strong interlayer coupling suppresses the macroscopic chimera due to the extreme transformation of the boundaries and the absence of regions of overlapping microscopic states in the control

parameter space. The provided analysis leads to the following conclusions. First, the macroscopic behavior of the multiplex network is strongly related to its dynamics on the microscopic level. Second, weak interlayer coupling with a small phase lag between the layers crucially transforms the network dynamics. As a results, a macroscopic chimera emerges in the neighborhood of boundaries between microscopic states, i.e., microscopic critical points. Additionally, we have proven the observation of the macroscopic chimeralike states in the finite-size multiplex network in the framework of Ott-Antonsen reduction.

The conducted research reveals a number of important issues. For instance, how does the heterogeneity of the multiplex network nodes affect the macroscopic state of the network and how does it influence the formation of macroscopic chimera? In this sense, the macroscopic chimera could be a relevant model for the description of multistable visual image perception performed by the human brain neural network and heterogeneity of the network elements could be associated with brain cognitive noise [37].

ACKNOWLEDGMENTS

We thank Professor Yuri Maistrenko for useful advices and valuable comments during the conduction of this research. This work was supported by Russian Science Foundation (Grant No. 17-72-30003).

[1] Y. Kuramoto and D. Battogtokh, Nonlinear Phenom. Complex Syst. **5**, 380 (2002).
[2] D. M. Abrams and S. H. Strogatz, Phys. Rev. Lett. **93**, 174102 (2004).
[3] M. J. Panaggio and D. M. Abrams, Nonlinearity **28**, R67 (2015).
[4] L. Larger, B. Penkovsky, and Y. Maistrenko, Nat. Commun. **6**, 7752 (2015).
[5] F. Böhm, A. Zakharova, E. Schöll, and K. Lüdge, Phys. Rev. E **91**, 040901 (2015).
[6] J. Hizanidis, V. G. Kanas, A. Bezerianos, and T. Bountis, Int. J. Bifurcat. Chaos **24**, 1450030 (2014).
[7] J. Hizanidis, N. E. Kouvaris, G. Zamora-López, A. Díaz-Guilera, and C. Antonopoulos, Sci. Rep. **6**, 19845 (2016).
[8] B. K. Bera, D. Ghosh, and M. Lakshmanan, Phys. Rev. E **93**, 012205 (2016).
[9] M. Santos, J. Szezech, F. Borges, K. Iarosz, I. Caldas, A. Batista, R. Viana, and J. Kurths, Chaos Soliton. Fractal. **101**, 86 (2017).
[10] M. R. Tinsley, S. Nkomo, and K. Showalter, Nat. Phys. **8**, 662 (2012).
[11] S. Nkomo, M. R. Tinsley, and K. Showalter, Phys. Rev. Lett. **110**, 244102 (2013).
[12] M. Wickramasinghe and I. Z. Kiss, PLoS One **8**, e80586 (2013).
[13] E. A. Martens, S. Thutupalli, A. Fourrière, and O. Hallatschek, Proc. Natl. Acad. Sci. USA **110**, 10563 (2013).
[14] T. Kapitaniak, P. Kuzma, J. Wojewoda, K. Czolczynski, and Y. Maistrenko, Sci. Rep. **4**, 6379 (2014).
[15] P. Jaros, L. Borkowski, B. Witkowski, K. Czolczynski, and T. Kapitaniak, Eur. Phys. J. Spec. Top. **224**, 1605 (2015).
[16] K. Blaha, R. J. Burrus, J. L. Orozco-Mora, E. Ruiz-Beltrán, A. B. Siddique, V. Hatamipour, and F. Sorrentino, Chaos **26**, 116307 (2016).
[17] J. Wojewoda, K. Czolczynski, Y. Maistrenko, and T. Kapitaniak, Sci. Rep. **6**, 34329 (2016).
[18] A. Zakharova, M. Kapeller, and E. Schöll, Phys. Rev. Lett. **112**, 154101 (2014).
[19] L. V. Gambuzza, A. Buscarino, S. Chessari, L. Fortuna, R. Meucci, and M. Frasca, Phys. Rev. E **90**, 032905 (2014).
[20] J. Hizanidis, N. Lazarides, and G. P. Tsironis, Phys. Rev. E **94**, 032219 (2016).
[21] A. Cardillo, J. Gómez-Gardeñes, M. Zanin, M. Romance, D. Papo, F. del Pozo, and S. Boccaletti, Sci. Rep. **3**, 1344 (2013).
[22] V. V. Makarov, A. E. Hramov, D. V. Kirsanov, V. A. Maksimenko, M. V. Goremyko, A. V. Ivanov, I. A. Yashkov, and S. Boccaletti, Sci. Rep. **7**, 17246 (2017).
[23] P. Holme, Phys. Rev. E **71**, 046119 (2005).
[24] C. Zhou, L. Zemanová, G. Zamora, C. C. Hilgetag, and J. Kurths, Phys. Rev. Lett. **97**, 238103 (2006).
[25] V. A. Maksimenko, A. Lüttjohann, V. V. Makarov, M. V. Goremyko, A. A. Koronovskii, V. Nedaivozov, A. E. Runnova, G. van Luijtelaar, A. E. Hramov, and S. Boccaletti, Phys. Rev. E **96**, 012316 (2017).
[26] E. A. Martens, Phys. Rev. E **82**, 016216 (2010).
[27] G. Bianconi, Phys. Rev. E **87**, 062806 (2013).
[28] M. Kivela, A. Arenas, M. Barthelemy, J. P. Gleeson, Y. Moreno, and M. A. Porter, J. Complex Netw. **2**, 203 (2014).
[29] S. Boccaletti, G. Bianconi, R. Criado, C. I. Del Genio, J. Gómez-Gardenes, M. Romance, I. Sendina-Nadal, Z. Wang, and M. Zanin, Phys. Rep. **544**, 1 (2014).
[30] S. Makovkin, A. Kumar, A. Zaikin, S. Jalan, and M. Ivanchenko, Phys. Rev. E **96**, 052214 (2017).
[31] V. A. Maksimenko, V. V. Makarov, B. K. Bera, D. Ghosh, S. K. Dana, M. V. Goremyko, N. S. Frolov, A. A. Koronovskii, and A. E. Hramov, Phys. Rev. E **94**, 052205 (2016).
[32] S. Ghosh and S. Jalan, Int. J. Bifurcat. Chaos **26**, 1650120 (2016).
[33] E. Ott and T. M. Antonsen, Chaos **18**, 037113 (2008).
[34] E. Ott and T. M. Antonsen, Chaos **19**, 023117 (2009).
[35] N. Marwan, C. M. Romano, M. Thiel, and J. Kurths, Phys. Rep. **438**, 237 (2007).
[36] F. P. Kemeth, S. W. Haugland, L. Schmidt, I. G. Kevrekidis, and K. Krischer, Chaos **26**, 094815 (2016).
[37] A. E. Runnova, A. E. Hramov, V. Grubov, A. A. Koronovsky, M. K. Kurovskaya, and A. N. Pisarchik, Chaos Soliton. Fractal. **93**, 201 (2016).